



## EXPERIMENTAL STUDY ON FOUR-SPAN RAHMEN BRIDGE WITH SLIDING-TYPE SEISMIC ISOLATION FOUNDATION

Tongxiang AN<sup>1</sup> and Osamu KIYOMIYA<sup>2</sup>

<sup>1</sup> *Research Associate of Advanced Res. Inst. for Sc. and Eng., Waseda University, Japan*

<sup>2</sup> *Professor, Dept. of Civil and Environmental Engineering, Waseda University, Japan*  
*Email: antongxiang@ybb.ne.jp*

### ABSTRACT :

In this study, the oscillation behavior and aseismicity of a 4-span Rahmen bridge with a sliding type seismic isolation foundation are investigated using model vibration experiments and numerical simulation. Built on Type III ground, the bridge is erected to 1/10 scale with a sliding-type foundation that was made by separating the footing in the horizontal direction, whereas conventionally piers and foundation structures are rigidly linked together. Teflon (PTFE) was inserted between the separated sections as the sliding interface material. The study results show that a sliding-type seismic isolation foundation has a significant positive effect in decreasing responses during earthquakes and the experimental results can be explained by the dynamic analysis.

**KEYWORDS:** sliding-type isolation foundation, Rahmen bridge, model vibration experiment, numerical simulation

### 1. PREFACE

Bridges serve as important constituent elements of highway and railway networks and, when damaged by earthquakes, have a direct negative effect on earthquake relief and reconstruction. Of particular note, the recent Northridge Earthquake of 1994, the Hyogoken-Nanbu Earthquake of 1995, the Taiwan Chi-Chi Earthquake of 1999, the Iran Earthquake of 2001, and the Chuetsu Earthquake of 2004 caused serious damage to many lifeline facilities, including aseismically-designed bridges. Triggered by such damage, aggressive research on the aseismicity of structures has led to notable developments in aseismic technology.

In bridge construction, seismic isolation structures have been actively adopted to appropriately prolong the natural period of structures and, at the same time, to divert seismic energy by means of dampers and other systems. In recent years, bearing-type seismic isolation systems have widely been adopted that inserted between superstructure girders and the bridge pier crest. In the U.S. and other nations, economical FPS (friction pendulum system) seismic isolation bearings have been developed and put into practical use. In Japan, rubber-type seismic isolation bearings have been extensively used that consists of damping hysteresis-type dampers and laminated rubber bearings that provide buffering. However, in cases when a bridge is constructed on soft ground and the bridge foundation is subjected to large ground deformation, seismic isolation bearings cannot accommodate the ground displacement. Further, because there is the danger of causing resonance with the ground, seismic isolation bearings are generally unsuitable and cannot be installed in Japan. As a result, a larger foundation structure is necessary, which in turn tends to increase the cost of construction.

A tall, slender structure is more stable in an earthquake due to its ability to rock in accordance with the earthquake motion (Housner, 1963). As for the spread foundations of bridges, the rocking motion associated with earthquakes causes the edges of the footings to separate from the ground (lift-off), thereby resulting in a decrease in earthquake energy (Kawashima, 2002). According to Mostaghel and Tanbakuchi, in cases where a structure is supported by a sliding device with low friction coefficient, seismic response acceleration is not affected by the frequency component of the input seismic force; accordingly, sliding-type seismic isolation devices can be applied regardless of the type of ground on which

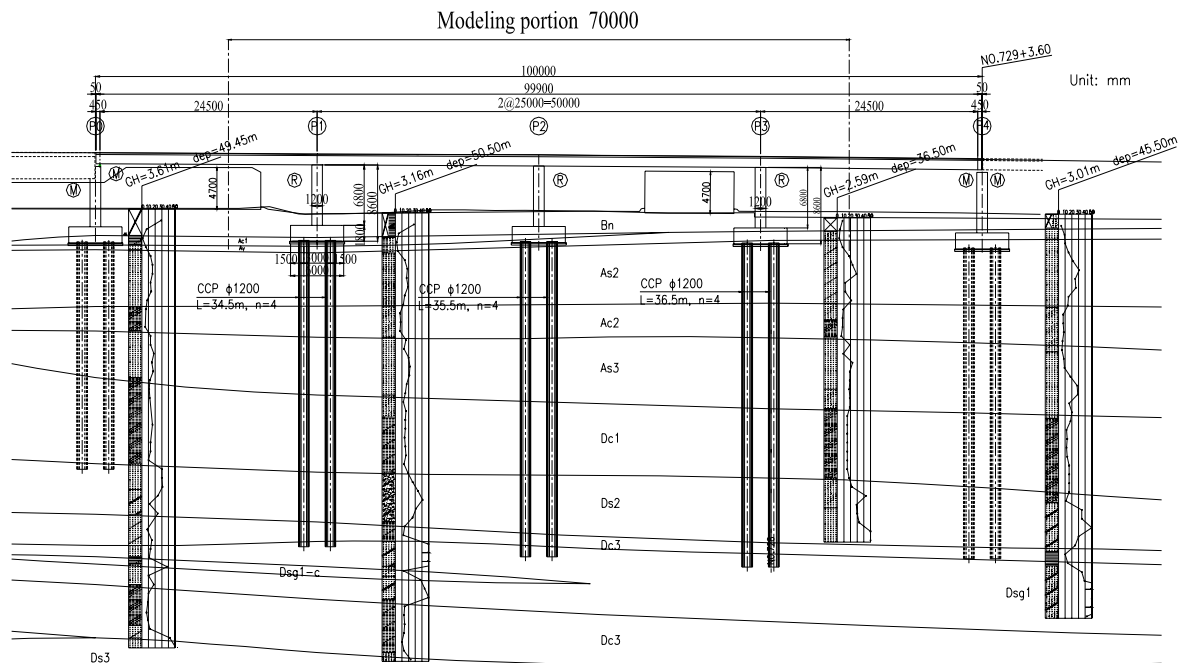


Figure 1 Outline of the prototype bridge

the bridges lie. Further, in the case of Greece's Rion-Antirio cable-stayed bridge that was completed in 2004, sand and gravel were laid between the pylon bottom and the ground, which was reinforced with steel pipe piles in order to reduce the seismic load by utilizing rocking and sliding of the base. When compared to the use of seismic isolation bearings, seismic isolation foundations designed to mitigate the seismic loads that work on a structure's foundation are thought to be of greater use, particularly for bridges consisting of RC or other heavy substructures. In their research, An et al. showed that a bridge pier in cases where the pier and its foundation are separated at the bridge pier footing and where isolating materials, such as sand, gravel or PTFE are inserted between the separated sections, based mainly on the use of relative displacement to absorb and dissipate earthquake energy, has an excellent aseismicity. In this study, an examination was made by means of model vibration tests on the vibration behavior and aseismicity of the structural system of a 4-span Rahmen bridge with Teflon inserted between the piers and their foundations.

## 2. OUTLINE OF EXPERIMENTS

### 2.1 Outline of Experimental Models

The experimental model was prepared by referencing a 4-span PC Rahmen bridge measuring 100.0 m in total length (25.0 m per span) and having a cast-in-place pile foundation with piles measuring 1,200 mm in diameter and about 35.0 m in length that was designed based on *Specifications for Highway Bridges* (published March 2002, Japan). The bearing support conditions in the longitudinal direction of the referenced bridge girders are M + R + R + R + M (M: movable; R: rigid). The ground consists of alternating layers of sand and clay, the base ground surface for seismic design is located at a depth of 50 m or more, and the ground is Type III as specified in *Seismic Design (Specifications for Highway Bridges, Japan*, hereinafter referred to as *Specifications V*). Fig. 1 shows an outline of the prototype bridge. In preparing the model, only the Rahman structure of the bridge's intermediate section, excluding the movement joint piers at the bridge end, was taken into account.

The similarity rate of the model is set at 1:10, and the density and acceleration are set at 1:1. The main similarity rates are shown in Table 1. Because it is difficult for the model dimensions to fully satisfy the similarity rate, as to the conventional structure (substructure and foundation structure

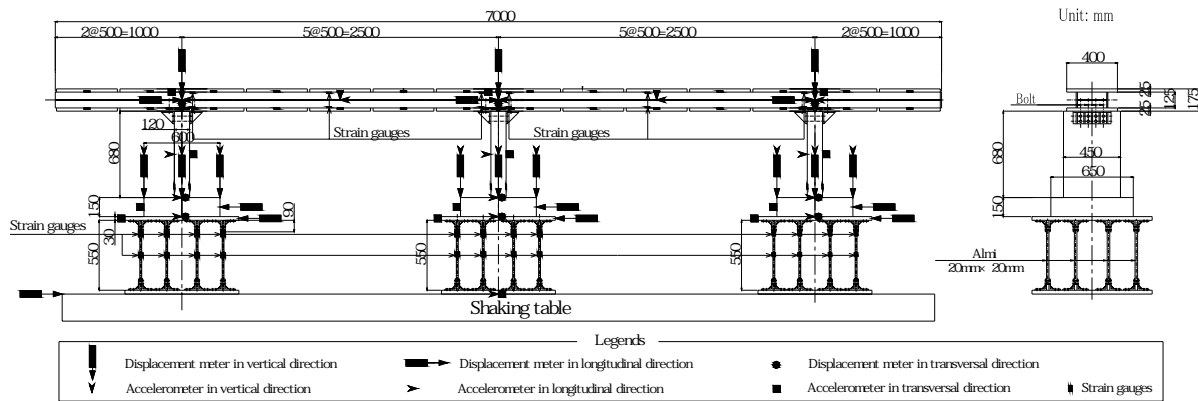


Figure 2 Outline of the experimental model and meters arrangement

Table 1 Main similarity rate

Item	Unit		Similarity rate	
Length	m	L	$\lambda$	$10^{-1}$
Mass	kg	M	$\lambda^3$	$10^{-3}$
Time	s	T	$\lambda^{0.5}$	$10^{-0.5}$
Density	kg/m <sup>3</sup>	M · L <sup>-3</sup>	$\lambda^0$	1
Acceleration	m/s <sup>2</sup>	L · T <sup>-2</sup>	$\lambda^0$	1
Force	N	M · L · T <sup>-2</sup>	$\lambda^3$	$10^{-3}$
Moment	N · m	M · L <sup>2</sup> · T <sup>-2</sup>	$\lambda^4$	$10^{-4}$
Young's Modulus	N/m <sup>2</sup>	M · L <sup>-1</sup> · T <sup>-2</sup>	$\lambda$	$10^{-1}$
Displacement	m	L	$\lambda$	$10^{-1}$
Rotation angle	rad		$\lambda^0$	1
Strain			$\lambda^0$	1
Stress	N/m <sup>2</sup>	M · L <sup>-1</sup> · T <sup>-2</sup>	$\lambda$	$10^{-1}$

Table 2 Primary nature frequency

		Longitudinal	Transversal direction
Prototype bridge A		1.97	2.04
Experimental model	Experimental value B	5.90	6.10
	Calculation value B'	5.73	6.28
	B'/B	0.97	1.03
Similarity rate B/A		3.00	2.99
Law of similarity		$10^{-0.5}=3.16$	

rigidly linked together), the model dimensions in this experiment were set by taking notice of the vibration behaviors of the structural system so that the following four conditions are satisfied: 1) mass of superstructure and bridge pier; 2) bending rigidity of the superstructure perpendicular to the bridge axis; 3) prominent primary natural frequency of the entire bridge system; and 4) maximum response acceleration and displacement.

The rigidity of the model superstructure was imparted by H-section beam (250 × 125 × 6 × 9 mm), and the mass was adjusted by supplementing steel sheets on the beam. Further, while the span length was set in conformity with the law of similarity, the length of girder overhang was set by taking into account the girder moment distribution condition during application of dead load. The bridge pier and footing were prepared using reinforced concrete, and their dimensions were decided according to the law of similarity. However, the width of the footing was set using Equation 2.1 so that the distance between the footing center and the position where the vertical reaction force acts would be less than 1/3 the footing width during a Level 1 earthquake. The pile foundation was made of aluminum bars which section, number, length, and arrangement were settled by taking notice only of the rigidity of the foundation. Fig. 2 shows an outline of the model, and Table 2 shows the primary natural frequency of the prototype bridge and the experimental model.

$$B_i \geq 3 \times k_h \times W_i \times h_i / V_i \quad (2.1)$$

Where,  $B_i$ : width of the  $i$ -th footing in excitation direction;  $k_h$ : lateral seismic design coefficient for Level 1 earthquake, here  $k_h=0.30$  (Type III ground);  $W_i$ : self weight of the  $i$ -th pier and the portion of the superstructure weight supported by the  $i$ -th pier;  $V_i$ : vertical load acting on the footing bottom of the  $i$ -th pier;  $h_i$ : acting height of  $W_i$  from the footing bottom of the  $i$ -th pier.

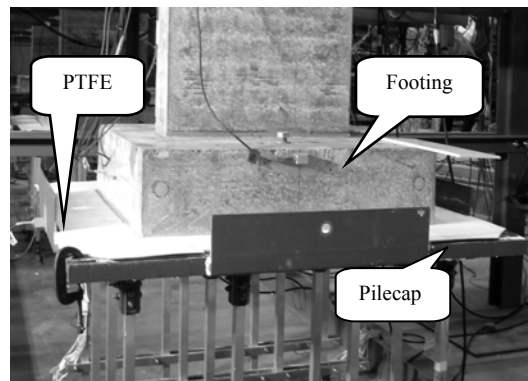


Figure 3 Schematic of the seismic isolation device

### 2.2 Seismic Isolation Foundation System

The seismic isolation foundation system was implemented by separating the pier from the foundation structure—both of which would conventionally have been rigidly linked by the footing—at the footing section and by inserting the seismic isolation material (sliding material, buffer material, etc.) between the separated sections. The term “sliding-type seismic isolation foundation” denotes a seismic isolation foundation to which a sliding material has been introduced as the seismic isolation material; in this case, the experimental seismic isolation material is Teflon sheets, that are 20% glass fiber. Each of the Teflon sheets was pasted to the lower surface of the footing and to the upper surface of the pilecap. Fig. 3 shows a schematic of the seismic isolation device. The friction coefficient is about 0.20. The adoption of a sliding-type seismic isolation foundation allows control over the vibration behavior of the structural system and over the upper limit of the horizontal load that is transferred to the foundation. The primary natural frequency  $f$  of the structural system vis-à-vis the sliding conditions can be expressed by Equation 2.2.

$$f = \sqrt{K_{h2} / M_u} / (2\pi) \quad (2.2)$$

Where,  $K_{h2}$ : stiffness of the isolation foundation system on sliding;  $M_u$ : structural mass above the isolation foundation system

The primary natural frequency under the sliding conditions of the structural system can be controlled by use of the restoring force of the seismic isolation system. In an extreme case in which the restoration force is not given, the natural frequency of the structural system becomes zero, and the seismic isolation effect vis-à-vis the seismic input with optional frequencies can be obtained regardless of the ground conditions. Further, the upper limit of the horizontal load  $H$  that is transferred from the bridge pier and superstructure, located above the seismic isolation system, to the foundation is shown in Equation 2.3. The maximum loads working on the foundation can be controlled by the friction coefficient and the restoration force of the seismic isolation system.

$$H = \mu V + K_{h2} \times \Delta x \quad (2.3)$$

Where,  $\mu$ : friction coefficient of the isolation foundation system;  $x$ : sliding displacement of the isolation foundation system.

### 2.3 Measurement Items and Meter Arrangement

Optical displacement gauges were attached to each footing and pedestal in the excitation direction and attached to both edges of each footing in vertical direction to measure the sliding displacement and the rocking of the seismic isolation system respectively. Accelerographs were attached to the pedestals, footings, gravitational center of the columns and superstructure to investigate the vibration behavior of the structural system. In addition, strain gauges were attached to the aluminum bars (piles), column reinforcements, and H-shapes that compose the superstructure (refer to Fig. 2).

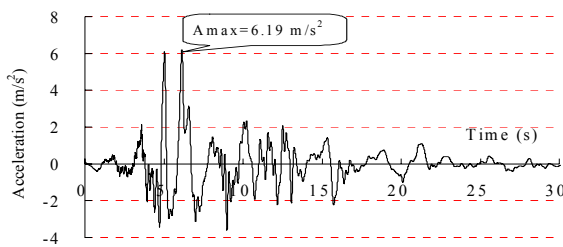


Figure 4 Experimental input wave (Port Island)

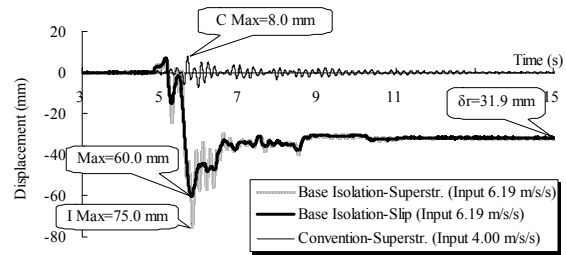


Figure 5-1 Response horizontal displacement

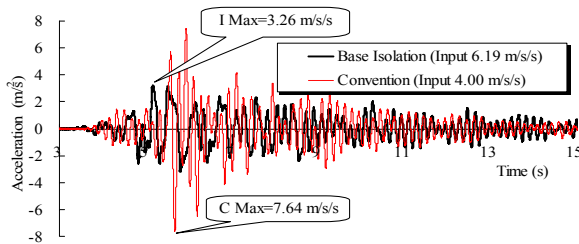


Figure 5-2 Response horizontal acceleration

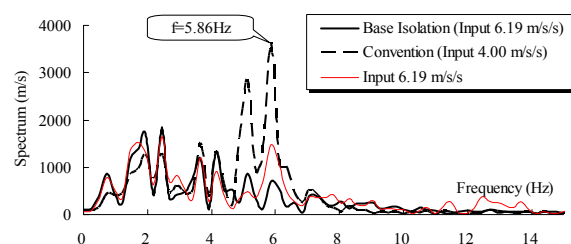


Figure 5-3 Fourier spectrum of acceleration

#### 2.4 Experimental Input Wave and Experimental Cases

The following earthquake wave form was selected as the input wave in this experiment. This wave form had the largest acceleration among those of Level 2 Type II seismic motion (inland earthquake) on Type III ground as specified in *Specifications V*—conditions that were recorded inland on Port Island during the Hyogoken-Nanbu Earthquake of 1995. Fig. 4 shows the wave form used in the experiment. The time interval of the input wave form was adjusted by the law of similarity. In order to grasp the relationship between the input amplitude and the vibration characteristics, sliding point, and other factors, the experiments were conducted by steadily increasing the amplitude by 1.0-m/s<sup>2</sup> increments to the maximum level.

Focusing on the structure of the footings, the experiment was conducted by roughly classifying as two types: a structure which the pier and its pile foundation rigidly linked at footing (conventional integrated structure), and a structure which the footing was separated in the horizontal direction and sliding material was introduced (seismic isolation structure). The experimental excitation was directed along both the bridge axis and perpendicular to it. Meanwhile, in the conventional integrated structure, the input wave amplitude was restricted to around 4.0 m/s<sup>2</sup> due to restrictions imposed on the model yield strength.

### 3. EXPERIMENTAL RESULTS AND EXAMINATIONS

Taking notice of the results obtained from bridge axis excitation to explain the response characteristics of the bridge and isolation effects of the isolation foundation system.

#### 3.1 Response Characteristics of Bridges

Fig. 5 shows an example of superstructure response values in the vicinity of the P2 bridge pier during bridge axis excitation (maximum input acceleration: 3.92 m/s<sup>2</sup> for the conventional structure, and 6.19 m/s<sup>2</sup> for the seismic isolation structure). While the maximum horizontal displacement of the conventional structure was 8 mm, that of the seismic isolation foundation structure was as much as 75 mm (60 mm in sliding displacement), or nearly 10 times that of the conventional type (refer to Fig. 5-1). This is mostly due to sliding of the seismic isolation device, which diverts the seismic energy by means of sliding displacement. It is believed that these phenomena are attributable to the fact that the seismic isolation device used in the experiment is of the sliding type and that the vibration of the structural system is mainly sliding vibration. Further, because the seismic isolation device is not subjected to restoration force, the seismic isolation structure does not exhibit reciprocating vibrations; and, the superstructure after being subjected to vibration retains a displacement of 31.9 mm, or about

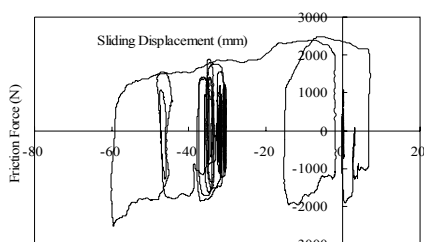


Figure 6 Friction force-sliding displacement

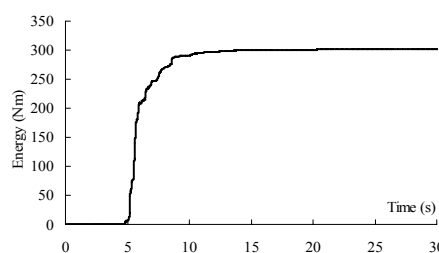


Figure 7 Cumulative energy absorption

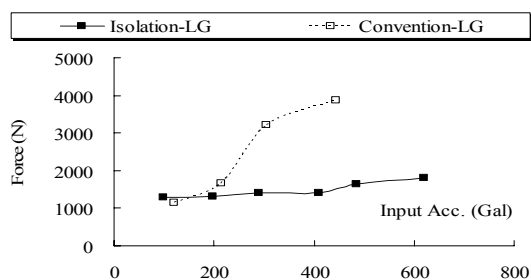


Figure 8-1 Axial force of pile

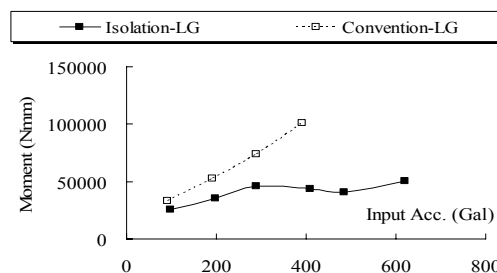


Figure 8-2 Bending moment of pile

1/20 the footing excitation-direction width (600 mm).

As regards the horizontal acceleration of the superstructure shown in Fig. 5-2, even though the maximum value of the input acceleration was increased to 1.58 times that of the conventional structure due to the introduction of the seismic isolation device, the maximum response value for the horizontal acceleration of the seismic isolation structure decreased to 0.43 times that of the conventional structure. As a result, an extremely large seismic isolation effect can be expected. Fig. 5-3 shows the Fourier spectrum of the superstructure's horizontal acceleration. The vibration of the conventional structure becomes prominent in the vicinity of its primary natural frequency ( $f=5.9$  Hz), whereas the seismic isolation structure vibrates in strict conformance to the input vibration characteristics and, at the same time, causes almost no amplification of the input vibration. It can be said from this data that the sliding-type seismic isolation structure shows little danger of causing resonance with the input seismic motion.

### 3.2 Behavior of Seismic Isolation System

With regard to the behavior of the seismic isolation system, studies were made on the hysteresis characteristics and the damping performance.

Fig. 6 shows an example of friction force-sliding displacement hysteresis loops (P2 bridge pier at maximum input amplitude). This friction force-sliding displacement hysteresis curve shows stable hysteresis characteristics and, as shown in Fig. 7, it is thought that the seismic isolation system has significant effect on absorption of earthquake energy.

### 3.3 Seismic Isolation Effects of Sliding-type Seismic Isolation Foundation

Study of the aseismicity of the seismic isolation foundation took notice of the sectional force of the foundation piles.

Fig. 8 shows an example of the sectional force of the P2 bridge pier foundation pile. As to the axial force of the pile (refer to Fig. 8-1), because there was almost no sliding of the seismic isolation device when the input amplitude was at around 100 gal, the response values for both the seismic isolation structure and the conventional structure were nearly identical. However, as the input amplitude increased, the axial force of the pile on the seismic isolation structure greatly decreased compared to that of the conventional structure, due to functioning of the seismic isolation device. When the input amplitude was at about 400 gal, the maximum axial force of the pile of the conventional structure reached 3,876 N, whereas the axial force of the pile of the seismic isolation structure decreased to as low as 1,799 N even when the input amplitude was as much as 619 gal. Further, the axial force of the

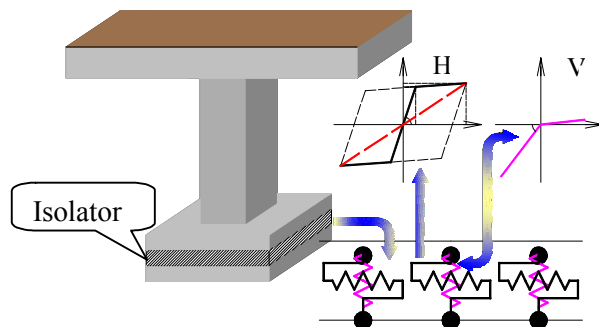


Figure 9 Model of the isolator

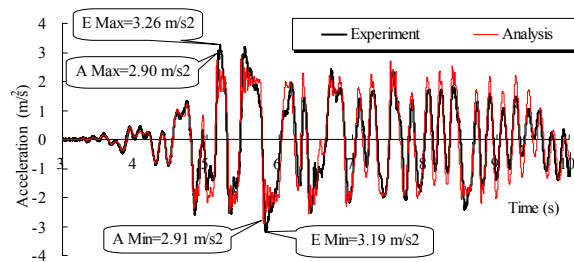


Figure 10-1 Acceleration of the superstructure

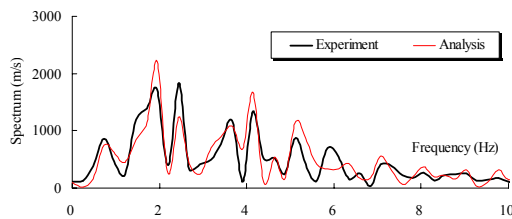


Figure 10-2 Fourier spectrum of acceleration

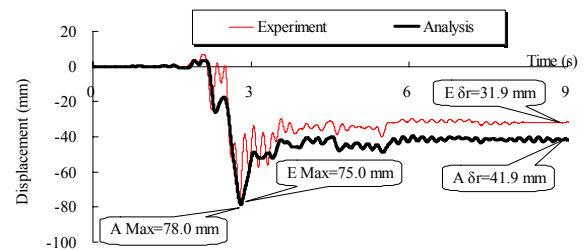


Figure 10-3 Displacement of the superstructure

pile of the seismic isolation structure was nearly flat and tended not to increase much even when the input amplitude increased; and, the maximum bending moment of the pile showed characteristics similar to those of the pile's axial force (refer to Fig. 8-2). It can be said from this data that a seismic isolation foundation can shut off loads brought about by great earthquakes while simultaneously improving the foundation's aseismicity.

#### 4. SIMULATION OF THE EXPERIMENTAL RESULTS

The test results are simulated by dynamic response analyses. The nonlinear dynamic analyses are performed by the direct integral calculus that the nonlinearity of a structural element can be taken in, and the integration is taken as the Newmark beta method. The superstructure, the pier columns and the piles of the experimental model are modeled to 3-D beam elements and, the footings and the pile-caps are modeled to 3-D solid elements. The isolator is modeled using spring elements in bridge axis direction and perpendicular to it and, vertical direction, respectively. The horizontal springs are of bi-linear to express the sliding and, the vertical springs are of nonlinear to express the lift-off of the isolation system as shown in Fig. 9. The friction coefficient of the isolation system is assumed to be 0.2. The stiffness of the isolation system is assumed to be in conformity with the oscillation mode of the test model measured by the free vibration test. In addition, the experimental input wave is used as the input acceleration wave.

The comparison results of the simulation and the experiment are shown in Fig. 10. As for the maximum (minimum) acceleration, the horizontal responses by the experiment and the analysis are 3.26 (3.19)  $m/s^2$  and 2.90 (2.91)  $m/s^2$ , respectively, as shown in Fig. 10-1. As to the accelerations, the analytical results are on the whole in agreement with the experimental results. The wave pattern for both the experiment and the analysis show much likeness. Fig. 10-2 shows the Fourier spectrum of horizontal acceleration at the superstructure. According to Fig. 10-2, it is clear that the oscillation behavior of the model is reproduced exactly by analysis. Fig. 10-3 shows that, as for the maximum horizontal response displacement of the superstructure, the experimental value is 75 mm and the analytical value is 78 mm. As for the residual displacement, the experimental value is 32 mm, and the analytical value is 42 mm. As for the displacements, the results of the analysis are roughly in agreement with the experimental results for both the maximum value and the wave form.

It is understood that the experimental results can be explained by dynamic analysis, thus the validity

of the analytical model in this study is confirmed by these comparisons.

## 5. Conclusions

The experimental model of this study was a 1/10 scale model of a four-span PC Rahmen bridge designed on Type III ground with a cast-in-place pile foundation. The foundation was isolated from the superstructure and the substructure by inserting into the separated footing a sliding-type seismic isolation device composed of PTFE (Teflon). Vibration tests were conducted on the model thus prepared, and the test results were simulated by dynamic analyses. These tests clarified the following:

- 1) In the seismic isolation structure discussed here, the response spectrum of the structural system nearly coincides with the input seismic motion spectrum due to sliding of the seismic isolation device, and vibrations can be controlled, thereby reducing the danger of resonance occurring between the bridge and the ground.
- 2) The seismic isolation device discussed here can secure stable friction force-sliding displacement hysteresis and efficiently absorb the energy of seismic motion, by means of which considerable damping effect can be expected.
- 3) The experimental results can be explained by the dynamic analysis. The validity of the analytical model considering nonlinear properties in this study is confirmed.

Application of an ordinary seismic isolation device in Type III and other types of soft ground is not recommended, but resonance between the bridge and the ground can be eliminated by the use of a sliding-type seismic isolation structure. While the displacement due to Level 2 seismic motion increases, the collision of girder ends can be prevented by installing appropriate expansion devices that allow the structural soundness of a bridge structure to be maintained. It was confirmed in the current experimental study that seismic isolation foundations are effective for Rahmen bridges.

In Rahmen bridges, the integration of superstructure girders and pier columns does not require bearings and, at the same time, allows for the substructure to bear part of the moment borne by the superstructure, thereby making it possible to reduce girder height. It is thought that the introduction of seismic isolation foundations will allow the realization of a new structural system that incorporates the advantages of both Rahmen and seismic isolation structures and that it will also allow the execution of more rational design. (However, in cases where the friction coefficient of the seismic isolation device is small, it will be necessary to install a shear key to constantly treat wind and other loads).

## REFERENCES

- Skinner RI, Robinson WH, McVerry GH (1993). An introduction to seismic isolation, John Wiley & Son U.K.
- Housner, G. W. (1963). The behavior of inverted pendulum structures during earthquakes. *Bulletin of the Seismic Society of America*. Vol. 53, pp. 403-417.
- Japan Road Association (2002). Specifications for Highway Bridge, Maruzen Japan
- N. Mostaghel and J. Tanbakuchi (1983). Response of sliding structures to earthquake support motion. *Earthquake Engineering and Structure Dynamics*, Vol.11, pp.355-366.
- Kawashima, K., Hosoiri, K. (2002). Effect of nonlinear rocking response of direct foundations on the hysteretic behavior of bridges, *Journal of Structural Mechanics and Earthquake Engineering, JSCE*, No. 703/I-59, pp. 97-111 (in Japanese).
- An, T., Kiyomiya, O. (2006). Dynamic response analyses and model vibration tests on seismic isolating foundation of bridge pier, *Journal of Structural Mechanics and Earthquake Engineering, JSCE*, Vol.62, No.3, pp.623-642.